

AD-A043 031

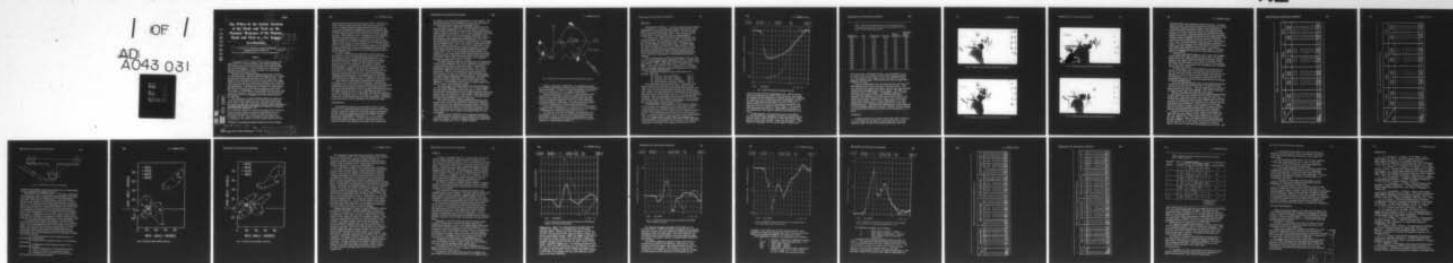
NAVAL AEROSPACE MEDICAL RESEARCH LAB DETACHMENT MICH--ETC F/G 6/19  
THE EFFECT OF THE INITIAL POSITION OF THE HEAD AND NECK ON THE --ETC(U)  
1975 C L EWING, D J THOMAS, L LUSTICK

UNCLASSIFIED

NL

1 OF 1

AD  
A043 031



END  
DATE  
FILMED  
9 -77  
DDC

AD A 043031

ADJ NO. DDC FILE COPY

6

11

751157

# The Effect of the Initial Position of the Head and Neck on the Dynamic Response of the Human Head and Neck to $-G_x$ Impact Acceleration

DDC  
REF ID: A66616

JUN 2 1977

10

C. L. Ewing, D. J. Thomas, L. Lustick, E. Becker  
G. Willems and W. H. Muzzy III

✓ Naval Aerospace Medical Research Laboratory Detachment

DDC  
REF ID: A66616  
A

11 1975

## Abstract

12 26p.

Several authors have  
In preparation of an analog of human head and neck, the reports by R. G. Snyder and others were noted which stated that initial position of the head and neck had a definite effect upon resulting response. An investigation was undertaken to attempt to quantitate this effect, as a part of a much larger study underway for several years.

Thirteen human volunteer subjects ranging from the 5th to the 97th percentile in sitting height were exposed to  $-G_x$  impact acceleration at peak sled accelerations of 6G and 10G. Two angles of the neck relative to chair and two angles of the head relative to the neck for a total of four conditions were tested for each subject for the 2 peak acceleration levels giving a total of 104 experiments. Instrumentation consisted of 6 accelerometers and two-axis rate gyro at the posterior spinous process of the first thoracic vertebral body, 6 accelerometers at the mouth, and a two-axis rate gyro at the top of the head. Three-dimensional photography from two orthogonally mounted onboard cameras was used also.

The input data at  $T_1$  along with the differential effects of initial head position relative to  $T_1$  on the linear acceleration at the origin of the head anatomical coordinate system and on the angular acceleration and angular velocity of the head will be presented along with the implications for modeling the response and a statistical comparison.

AN EXTENSIVE SERIES OF Army-Navy-Wayne State University human volunteer impact acceleration experiments have been conducted and reported in which the head and neck were instrumented (1-5). \* Input accelerations were limited to the  $-X$  direction of the seated, nominally upright subject and were

\*Numbers in parentheses designate References at end of paper.

we → 391 221

further limited to peak sled acceleration of 10G. Although the initial angular and linear position of the head and the first thoracic vertebral body were approximately constant from run to run and documented by photography no exact prepositioning procedure was used and no effort was made to analyze the effect of initial angular position of the head and neck on the dynamic response. From reports of other investigators and from modeling the human dynamic response, it is expected that the initial angular position of the head relative to the neck and the neck relative to the torso will have an effect on the measured dynamic response of the human volunteer subjects (6, 7). For the present study, a series of 100 runs on 13 volunteer subjects was completed to measure this effect, using newly developed instrumentation and photographic mounts at the new Navy Acceleration Laboratory in New Orleans.

Precision tracking of the head relative to the neck and both relative to the seat during dynamic events requires the use of coordinate systems. Coordinate systems based on x-ray anthropometry were established on the first thoracic vertebra (T<sub>1</sub>) and on the head. Other coordinate systems used were those for the sled, the laboratory, the cameras, and the instrumentation. By use of the anatomical coordinate systems, it was possible to establish with precision the location and orientation of T<sub>1</sub> relative to the sled, the head relative to the sled, and thus the head relative to T<sub>1</sub> and to the laboratory reference coordinate system. This approach further permitted establishment of the angles of head with respect to neck and neck with respect to laboratory prior to imposition of acceleration.

High precision accelerometer packages were mounted on the human at T<sub>1</sub>, on the head and on the sled. Accelerations measured by the human mounts were transformed into the anatomical coordinate systems using the equations of rigid body mechanics, thus permitting normalizing of input and output data between subjects. The head has been shown to act as a rigid body previously (5). T<sub>1</sub> itself is assumed to act as a rigid body, and therefore represents input to the vertebral column of the head-neck system, independent of restraint, except for that portion of the acceleration transmitted by the soft tissues, which is estimated to be relatively small.

## DEFINITIONS

The geometrical position and orientation of the T<sub>1</sub> mount relative to T<sub>1</sub> anatomical coordinate system and the mouth mount relative to the head anatomical coordinate system was measured for each subject by adapting previously developed two-dimensional x-ray anthropometry techniques (4, 5, 11) to a three dimensional configuration. A lateral view and an anterior view of the subject is taken while he is fixed relative to two cassettes fixed at right angles to each other with a lateral and



an anterior x-ray tube fixed perpendicular to the cassettes. The three-dimensional x-ray techniques were used for reduction of the three dimensional sensor and photographic data.

The head and T<sub>1</sub> anatomical coordinate systems have been defined for this organization (11). For the head, the origin is at the midpoint of the line connecting the left and right external auditory meatus lead markers. The +X axis is defined by the origin and the midpoint of the line connecting the infraorbital notch lead markers. The +Z axis is in a cephalad direction normal to the Frankford plane defined by the lead markers. The +Y is toward the left ear normal to the X, Z plane which is considered the mid-sagittal plane. For T<sub>1</sub>, the origin is at the center of the anterior superior corner of T<sub>1</sub>. The +X axis is defined by a line from a point midway between the superior posterior corner and inferior posterior corner of the posterior spinous process of T<sub>1</sub> to the origin. The +Y axis is through the origin along a line parallel to a line from a point at the articular facet of the right transverse process, right first-rib articulation to the same point on the left. The +Z axis is from the origin in the cephalad direction perpendicular to the X, Y plane.

The basic reference frame for the entire series of experiments is fixed to the laboratory (12). This is defined by first defining a sled coordinate system in which the origin is a benchmark permanently machined into the sled structure. The +X axis is parallel but opposite in direction to the thrust vector of the accelerator. The +Z axis is parallel to gravity and positive upward and the +Y axis is such that the sled coordinate system is a right-handed orthogonal coordinate system. The laboratory coordinate system is coincident with the sled coordinate system prior to sled motion and remains fixed relative to the laboratory. All coordinate systems used are right-handed where the X, Y and Z axes are taken in order.

The head angle is the angle between the head anatomical +X axis and the laboratory +X axis (Fig. 1). In order to define the neck angle a line from the anterior superior corner of the first thoracic vertebral body (T<sub>1</sub>) to the head anatomical coordinate system origin was constructed. Neck angle is the angle between this line and the laboratory +Z axis (Fig. 1). Only the initial condition values of these angles are presented.

All of the kinematic variables presented have been transformed to the origin of the head and T<sub>1</sub> anatomical coordinate systems relative to the laboratory coordinate system. The zero time displayed on the figures is 40 ms before first motion of the sled as determined by an analysis of the sled acceleration data, which projects the rate of onset of acceleration back to zero acceleration.

Angular velocity (RM2OXS) is the component around the +Y head anatomical coordinate system relative to the laboratory coordinate system. In these -X impact acceleration experiments there is no significant +X or +Z angular velocity.



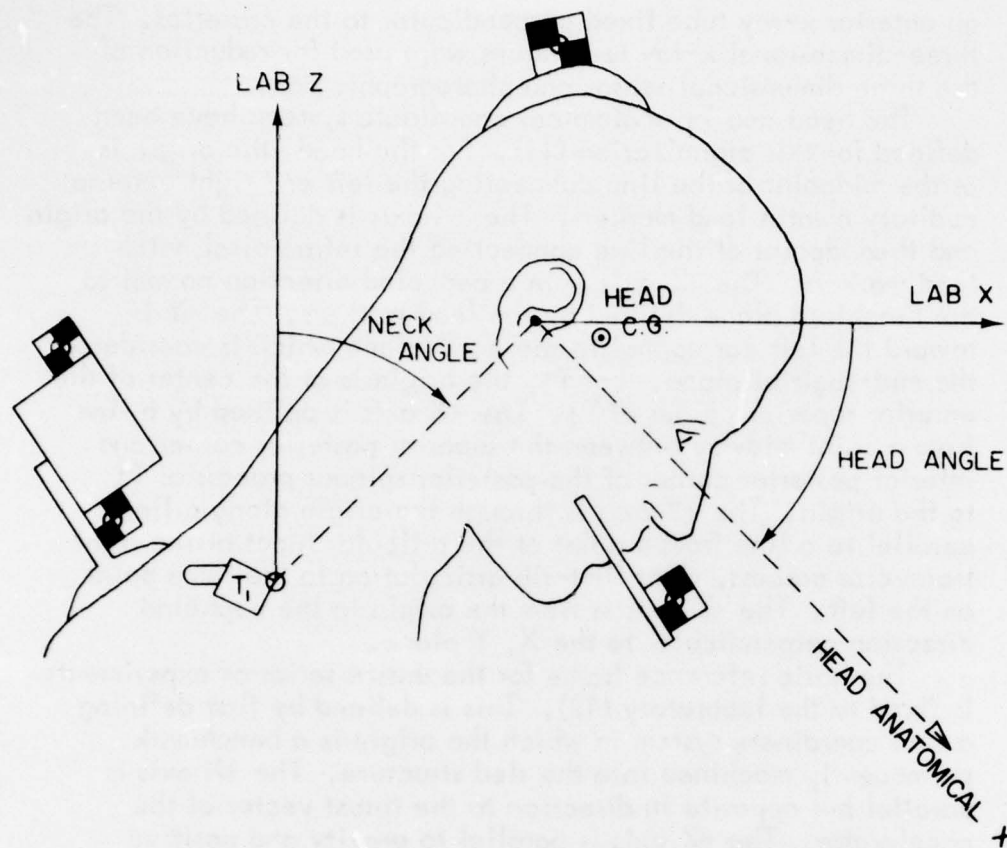


Fig. 1 - Illustration of the initial conditions of head angle and neck angle

Angular acceleration (QM2OXS) is the component around the +Y head anatomical coordinate system relative to the laboratory coordinate system. In these -X impact acceleration experiments there is no significant +X or +Z angular acceleration.

Resultant acceleration (AMXZOS) is the magnitude of the acceleration at the head anatomical coordinate system origin relative to the laboratory coordinate system origin computed from the components along the X and Z axes of the laboratory coordinate system. Under these -X impact acceleration experiments the Y component of acceleration is insignificant.

Horizontal acceleration at T<sub>1</sub> (ATXXOS) is the acceleration component of the T<sub>1</sub> anatomical coordinate system origin relative to the laboratory coordinate system along its X axis.

All units are in the meter, kilogram, seconds system with the exception that G is also used to express acceleration and centimeters are used to express certain anthropometric values. The runs are identified by a number beginning with LX and the subject by a number beginning with H.

## METHODS

**EXPERIMENTAL DESIGN** - Thirteen volunteer human subjects were exposed to two controlled sled acceleration profiles in four conditions of initial head and neck position. The total number of runs required by this design is 104. One volunteer left the program early, therefore, only 100 runs were completed.

A twelve-inch (.3048 m) Bendix HyGe<sup>®</sup> accelerator was used to accelerate a 1.2 meter by 3.7 meter rail mounted sled, of 1669 Kg mass. The accelerator stroke is limited to five feet and the effective drag is about 0.2G. The sled coasted to a stop for the 6G runs within 13.7 meters and for the 10G runs within 35 meters on the 213 meter track. The long track permitted imposition of the experimental acceleration pulse at the beginning of the run with no intervening braking pulse which would have confounded the telemetered physiological response.

The two acceleration profiles are illustrated in Fig. 2. The first is characterized by peak acceleration of  $60 \pm 1 \text{ m/sec}^2$  (6G), rate of onset of  $3800 \pm 500 \text{ m/sec}^3$  and duration above 75% of the peak of  $119 \pm 3 \text{ ms}$ , and the second  $101 \pm 1 \text{ m/sec}^2$  (10G),  $8000 \pm 700 \text{ m/sec}^3$  and  $113 \pm 1 \text{ ms}$ , respectively. The subjects were restrained by shoulder straps and lap belt with an inverted vee in an upright seated position.

Four conditions of head and neck initial position are defined. They are:

- |                                    |        |
|------------------------------------|--------|
| (a) Neck up, chin up (NUCU)        | Fig. 3 |
| (b) Neck up, chin down (NUCD)      | Fig. 4 |
| (c) Neck forward, chin up (NFCU)   | Fig. 5 |
| (d) Neck forward, chin down (NFCD) | Fig. 6 |

The experiments were confined to the -X direction of the subject with the same seat as that previously used at Wayne State University and a restraint system of the same geometry with wider straps. From these previously reported runs the head and neck response was demonstrated to be confined to the mid-sagittal plane of the man, which moved in the X, Z plane of the laboratory. Therefore, only the mid-sagittal plane data are presented and analyzed. The volunteer subjects were young U. S. Navy active duty enlisted males. The range of anthropometry is described by the selected measures listed in Table 1 (8, 9).

**EXPERIMENTAL MEASUREMENTS** - The dynamic response of each subject was measured using six piezoresistive accelerometers mounted on a T shaped (T) plate at the mouth and six accelerometers mounted to a T plate over the T<sub>1</sub> posterior spinous process. The standard geometry of the T plate is illustrated in Fig. 7, showing the position and orientation of the accelerometers (10). The output of each accelerometer was hardwired to an EAI-Pacer 600<sup>®</sup> hybrid computer, digitized at 2000 samples per second and stored on magnetic disk in real time. The calibration information is available in the computer memory prior to the

LX0711	AC1LOS = (+)	H00041	59.	3743.9
LX0567	AC1LOS = (.)	H00041	100.	7281.1

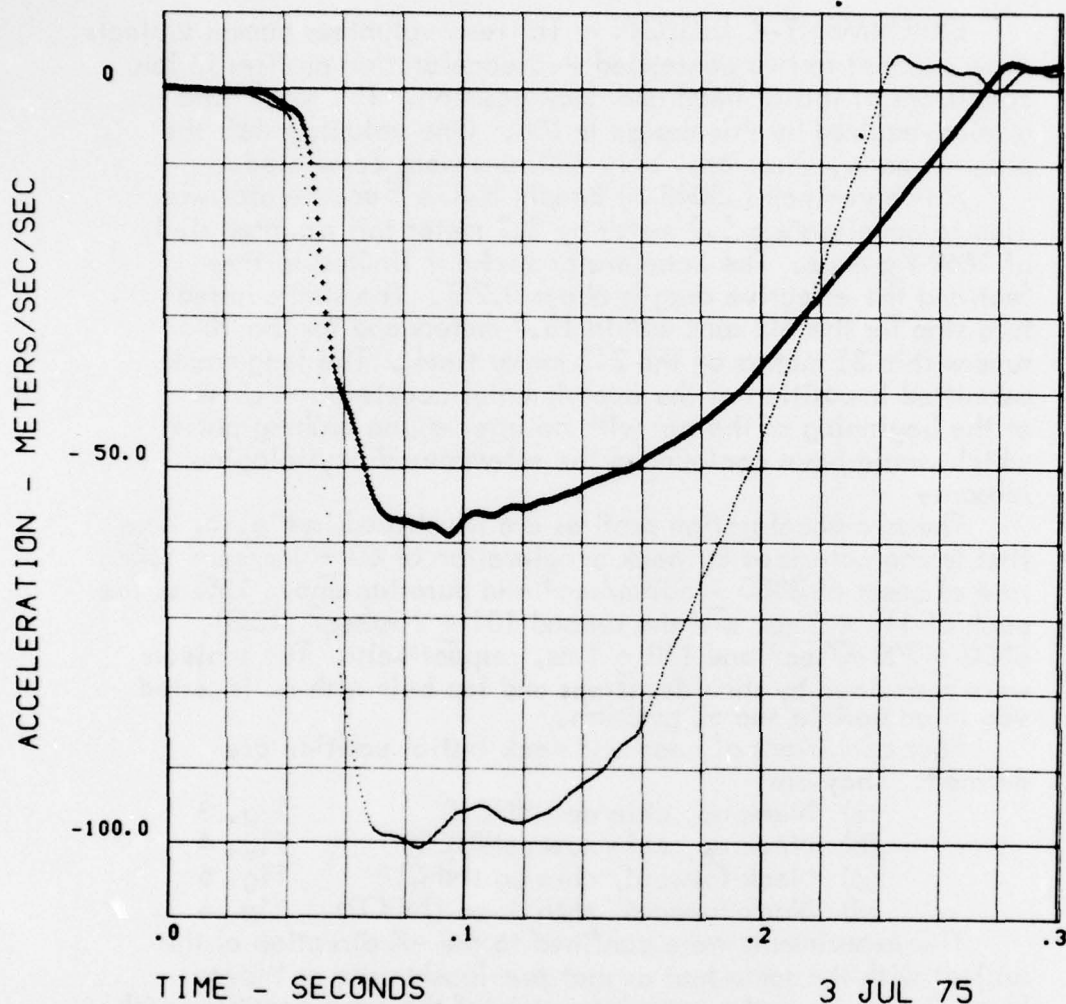


Fig. 2 - Typical sled acceleration profiles (6 and 10G)

run and carried with the accelerometer data. Within minutes after each experiment the digital data are scaled, reconverted to analogue form and plotted on a cathode ray tube for validation by comparison with a scaled light beam oscillographic plot of the data independently generated at the time of the run. In addition there was a two axis rate gyroscope mounted on the head mount and one mounted on the T<sub>1</sub> mount. The data from these gyroscopes was used as an independent measurement of two components of the angular velocity of the head and of the neck.

Cinephotographic coverage of the event is provided by two sled-mounted, pin-registered 16 mm five hundred frame per second cameras, Milliken DBM 5D or DBM 55<sup>®</sup>, situated orthogonally to each other at about 1 meter from the subject. These cameras are equipped with 12.5 mm Kinoptic<sup>®</sup> lenses at f4.



Table 1 - Selected Anthropometric Data on 13 Volunteer Subjects from C. Clauser and K. Kennedy (8). The Percentile Sitting Height is referenced to the U. S. Naval Aviator Population (9)

SUBJECT NO.	AGE	STATURE (cm)	MASS (Kg)	SITTING HEIGHT (cm)	PERCENTILE SITTING HEIGHT
H029	19	178.4	98.4	91.6	45%
H032	21	174.6	73.9	92.0	50%
H033	20	176.4	93.9	96.4	93%
H034	20	174.0	83.9	90.6	33%
H035	22	184.4	88.9	98.4	97%
H037	20	181.7	71.7	95.0	84%
H038	20	164.9	60.3	87.0	05%
H039	20	172.5	73.0	93.0	63%
H041	20	182.0	77.6	90.2	27%
H042	21	177.1	74.8	92.3	53%
H043	21	178.0	64.4	95.5	87%
H044	19	175.8	66.2	93.2	64%
H045	19	175.4	73.9	93.4	66%

Each camera has a 140 degree shutter, and is equipped to print ten digits of the time of day at time of shutter opening resolved to 0.1 ms along the frame edge as well as serial IRIG B timing along the opposite edge. One-hundred foot rolls of Kodak 2479 RAR film are used.

Lighting is provided by four sled-mounted General Electric® 4582 lamps mounted in pairs at each of the camera sites. One was mounted to the right of the subject with lens axis approximately normal to the mid-sagittal plane of the subject. The other was mounted in front of the subject. Photographic targets on the T<sub>1</sub> instrumentation mounts as well as the sled-mounted target remained in the field of view of the lateral camera (Fig. 3 - 6). Targets on the mouth instrumentation mount were in the field of view of both cameras. The T<sub>1</sub> mount displacement in the mid-sagittal plane of the subject was measured relative to the sled coordinate system. The mouth mount displacement can be measured in three dimensions relative to the sled. However, for this analysis it was assumed that all motion occurred in the mid-sagittal or X, Z plane.

## ANALYSIS

DETERMINATION OF INITIAL HEAD AND NECK ANGLES - X-ray anthropometry provides the vector location of the instrumentation origin as well as the transformation matrix from the



Fig. 3 - Example of neck up, chin up (NUCU) initial condition



Fig. 4 - Example of neck up, chin down (NUCD) initial condition



Fig. 5 - Example of neck forward, chin up (NFCU) initial condition



Fig. 6 - Example of neck forward, chin down (NFCD) initial condition



instrumentation to the anatomical coordinate system. The photo analysis program uses these anthropometric data together with the fixed known location of photo targets in the instrumentation coordinate system; fixed known location of the sled mounted cameras in the sled coordinate system; the transformation matrix between the camera coordinate systems and the sled coordinate system; and the measurement obtained from the photographic data of photo targets to establish the vector location of the head anatomical origin displacement and the T<sub>1</sub> origin relative to the sled, which can then be related to the laboratory coordinate system. This same program also establishes the orientation of the head anatomical coordinate system and the T<sub>1</sub> anatomical coordinate system relative to the laboratory system. The photo data was automatically digitized by a photo digitizing system (PDS Series 200<sup>®</sup>).

The photo data from 4 targets on the T<sub>1</sub> mount and 4 targets on the mouth mount from the lateral camera only were used to obtain the initial conditions by analyzing 15 frames, approximately 2 msec apart, prior to first motion of the sled to verify that there was little head or neck motion prior to this condition. The initial values are consistent with the position and orientation data at about first motion.

The least square fit of initial conditions was obtained consistent with the photo data and consistent with the constraint that the anatomical origins were only allowed to be moved in the laboratory X and Z directions and the rotation was only about the laboratory Y axis. This constraint is consistent with the established finding that motion of the head and neck was limited to the mid-sagittal plane.

The neck angle illustrated in Fig. 1 was calculated from the coordinates of the head anatomical and T<sub>1</sub> anatomical origin locations at first sled motion. The head angle shown also in Fig. 1 comes directly from the photo program. Only initial conditions of head and neck angle are presented in this report.

Tables 2 and 3 show the neck and head angle thus determined for each subject for each condition for the 6G and 10G runs respectively. Observation of the mean angles for each condition in which the subject was asked to place himself show that on the average over all subjects, the orientation was consistent with the description for that condition. Close inspection of the table reveals that there is a large variation between subjects and that there are some inconsistencies especially in head orientation between the descriptor and the actual measured orientation.

Figures 8 and 9 show the initial values of neck angle and head angle for each subject for each condition for the 6G and 10G runs respectively. These figures illustrate the variation between subjects as well as the approximate clustering obtained for each condition. Of particular note is that the clustering for the 6G and 10G runs is very similar and that the chin down position allows for a much more forward position of the neck. The

Table 2 - Initial Neck and Head Angle (Degrees) (6G runs)

Cond Subj	NFCU		NFCU		NUCD		NUCU	
	Neck Angle	Head Angle	Neck Angle	Head Angle	Neck Angle	Head Angle	Neck Angle	Head Angle
29	42.40	-4.35	54.52	47.32	-1.53	-2.57	20.61	1.31
32	40.19	-12.89	85.22	72.85	9.35	10.02	20.69	-10.47
33	49.52	-1.17	84.24	57.59	19.16	19.92	23.90	1.92
34	52.56	-32.47					16.82	-9.31
35	75.73	7.54	55.75	57.22	8.74	7.52	19.77	9.42
37	47.12	-2.84	90.58	67.25	18.51	6.01	25.08	-2.85
38	70.94	4.75	66.75	78.27	14.03	-4.06	18.98	6.11
39	46.73	-8.56	65.74	58.14	-4.59	-12.97	12.94	-16.06
41	22.94	-9.59	33.35	82.50	17.30	26.70	18.01	-2.91
42	48.69	-1.47	84.94	75.26	18.41	7.14	20.07	2.37
43	76.80	1.62	53.75	52.42	1.33	-3.62	18.95	-1.16
44	45.96	-4.7	74.85	54.17	18.34	5.51	24.56	5.01
45	47.65	11.16	84.00	69.45	27.20	14.22	22.58	-1.12
Mean	43.29	-3.74	79.13	66.04	12.19	6.15	20.22	-1.29
St'd Dev	6.55	10.10	13.68	10.65	9.67	11.02	3.35	7.15

Table 3 - Initial Neck and Head Angle (Degrees) (10G runs)

Cond Subj	NFCU		NFCU		NUCD		NUCU	
	Neck Angle	Head Angle	Neck Angle	Head Angle	Neck Angle	Head Angle	Neck Angle	Head Angle
29	50.54	.66	73.20	55.28	20.64	18.70	27.58	-4.54
32	45.25	9.66	37.71	38.24	14.01	-2.96	11.30	-16.25
33	46.27	-7.63	79.60	58.66	3.17	6.39	20.35	5.62
34	27.05	.69					10.16	-13.46
35	76.23	7.04	42.05	50.07	9.55	10.80	19.59	8.24
37	70.13	1.34	43.83	38.07	17.35	4.79	21.19	-5.90
38	41.55	-6.81	30.71	57.70	14.53	10.10	20.90	4.54
39	51.01	11.27	83.08	70.32	-4.26	-9.88	5.54	-20.35
41	37.10	1.20	35.25	79.24	5.43	8.68	21.08	8.60
42	51.67	20.76	72.12	67.45	15.59	8.25	26.83	6.89
43	31.42	-3.56	48.50	45.69	4.39	-7.26	28.21	-1.36
44	45.07	6.06	58.10	45.92	18.25	6.82	32.59	10.68
45	55.05	29.64	48.41	73.13	35.82	27.97	30.78	10.03
Mean	45.07	4.32	74.08	64.18	12.90	6.87	21.28	-1.48
Std Dev	10.06	10.96	15.59	13.10	10.32	10.43	8.27	10.68



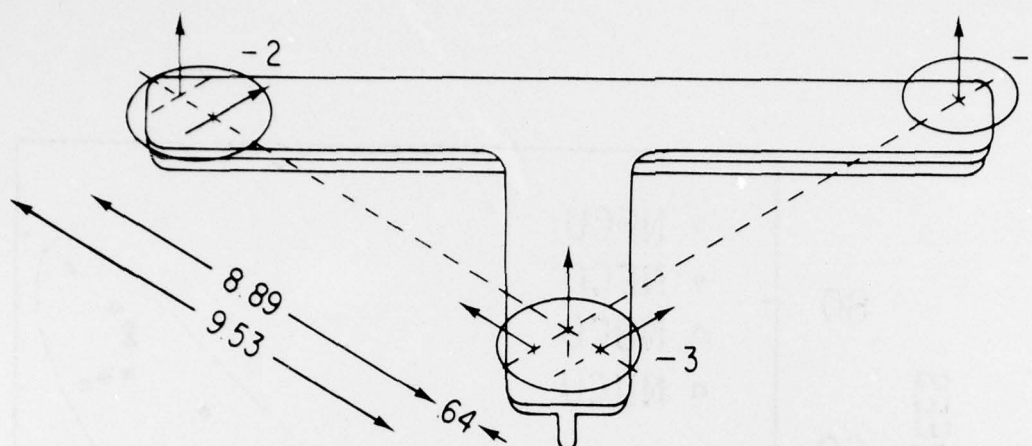


Fig. 7 - 6 accelerometer system 3-2-1 configuration

data base encompasses a wide range of both neck and head angles, which is important for regression analysis.

**PROCESSING OF SENSOR DATA** - The linear accelerations and the angular velocity and accelerations presented in this paper were determined from a configuration of six accelerometers on the mouth T plate and six accelerometers on the neck T plate. The canonical configuration of these accelerometers are shown in Figure 7. The selection of this configuration and its performance during these experiments is presented by Becker and Willems (10). The orientation, bias, and sensitivity of each accelerometer in the configuration is determined from data obtained by mounting each T plate configuration on a rate table in six or more different orientations. Subsequent to the run, the constants determined in the calibration procedure are employed to obtain scaled accelerometer data for each of the accelerometers in the configuration (10).

This scaled accelerometer data together with the position and orientation data of each accelerometer in the instrumentation system, the transformation from the instrumentation to anatomical system, the location of the instrument origin relative to anatomical origin, and the initial quaternions defining the initial orientation of the anatomical system relative to the laboratory fixed system allow for the determination of the following variables as a function of time.

- (a) Linear acceleration of the anatomical origin in the laboratory fixed system.
- (b) Velocity of the anatomical origin in the laboratory fixed system.
- (c) Displacement of the anatomical origin in the laboratory fixed system.
- (d) Angular acceleration in the anatomical system.
- (e) Angular velocity in the anatomical system.
- (f) Orientation of the anatomical axes relative to the laboratory fixed coordinate system.

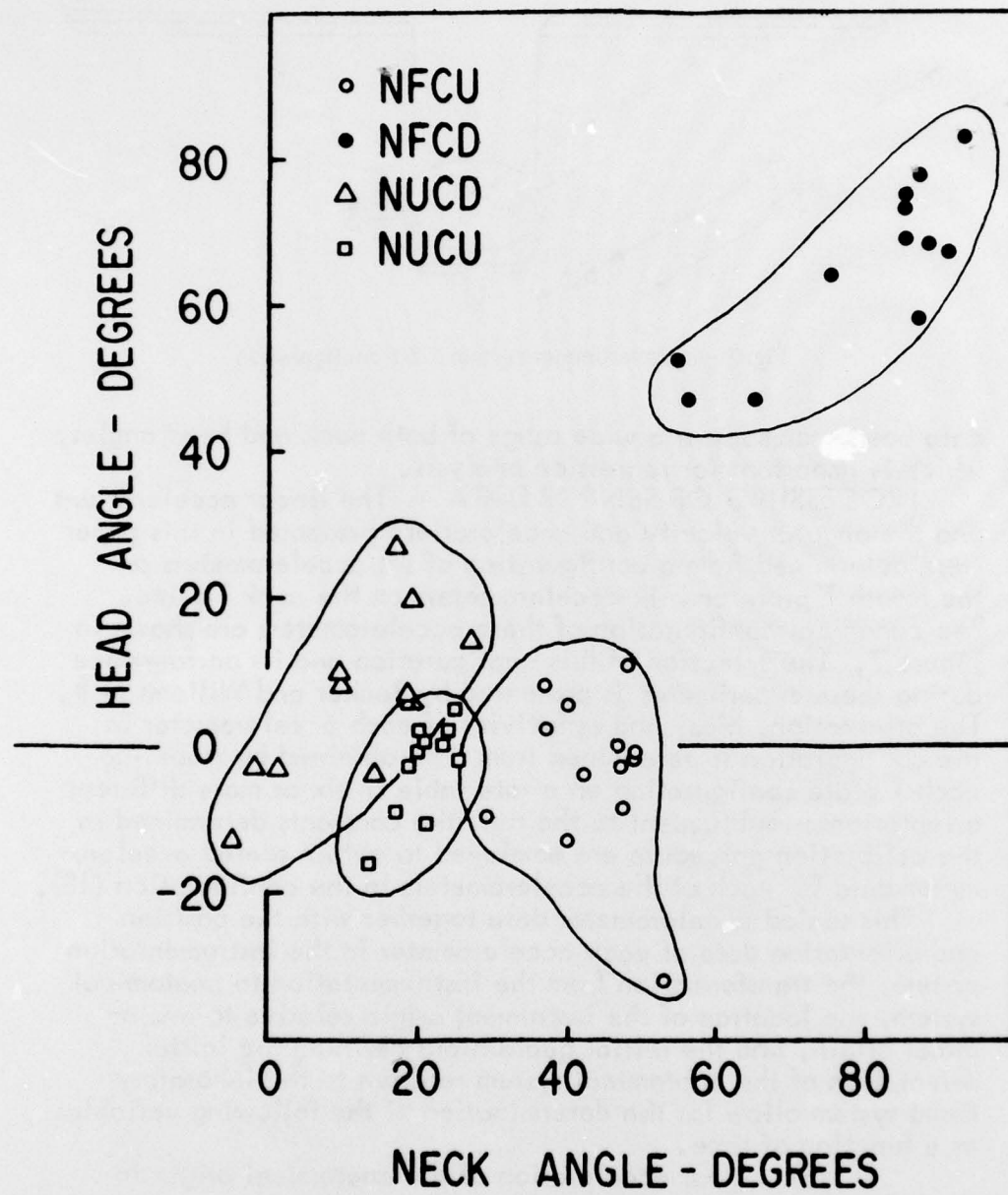


Fig. 8 - Clustering of initial conditions (6G runs)

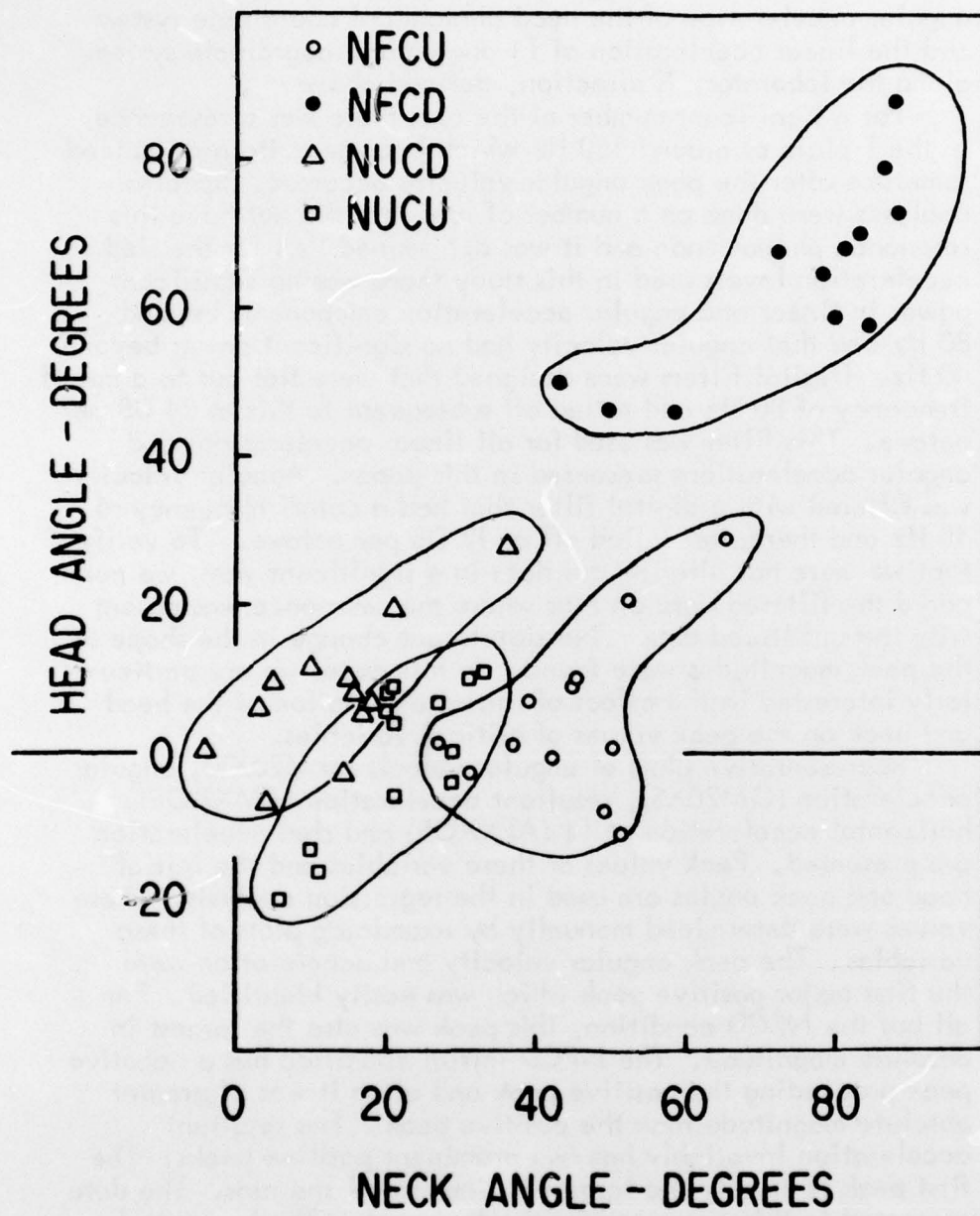


Fig. 9 - Clustering of initial conditions (10G runs)



The algorithm for obtaining these parameters is described by Becker and Willems (10). The variables selected for this analysis are linear acceleration magnitude, angular velocity and angular acceleration of the head anatomical coordinate system and the linear acceleration of T1 anatomical coordinate system along the laboratory X direction, defined above.

For a significant number of the runs there was a resonance in the T plate at around 150 Hz which became quite pronounced sometime after the peak angular velocity occurred. Spectral analyses were done on a number of runs that did not have this resonance phenomenon and it was determined that for the sled acceleration levels used in this study there was no significant power in linear and angular acceleration components beyond 80 Hz and that angular velocity had no significant power beyond 40 Hz. Digital filters were designed that were flat out to a cutoff frequency of 80 Hz and rolled off subsequent to this at 24 DB per octave. This filter was used for all linear accelerations and angular accelerations presented in this paper. Angular velocity was filtered with a digital filter that had a cutoff frequency of 40 Hz and thereafter rolled off at 12 DB per octave. To verify that we were not altering our data in a significant way, we compared the filtered data on runs where the resonance was absent with the unfiltered data. No significant change in the shape or the peak magnitudes were found. In this paper we are particularly interested in the effect of initial orientation of the head and neck on the peak values of critical variables.

Representative plots of angular velocity (RM20XS), angular acceleration (QM20XS), resultant acceleration (AMXZOS), horizontal acceleration at T1 (ATXXOS) and sled acceleration are presented. Peak values of these variables and the initial head and neck angles are used in the regression analysis. These values were determined manually by examining plots of these variables. The peak angular velocity and acceleration were the first major positive peak which was easily identified. For all but the NFCD condition, this peak was also the largest in absolute magnitude. The NFCD initial condition has a negative peak preceeding the positive peak and often it was of greater absolute magnitude than the positive peak. The resultant acceleration invariably has two prominent positive peaks. The first peak is usually the largest but not in all the runs. The data presented in this paper are for the first peak. The horizontal acceleration at the T1 origin is predominantly negative and has two peaks. The data presented in this paper are for the first peak which is almost invariably the largest. Tables 3 and 4 summarize the peak values obtained for each of the variables for each condition and subject for the 6 G and 10 G runs respectively.

## RESULTS

In Figure 10 through Figure 13, a typical 10G run from the NUCU initial condition is compared with a typical 10G run from the NFCD initial condition. These two conditions represent the extremes of the initial condition excursions examined in this paper. Observation of the figure comparing angular velocities shows a dramatic change in both shape of the profiles as well as the peak values (Fig. 10). The peak angular velocity from the NFCD initial condition is less than  $1/2$  of that from the NUCU initial condition. In addition for the NFCD condition, the first positive peak is preceeded by a negative peak which for some runs is larger than the positive peak. The positive peak of NFCD lags that of NUCU by approximately 12 msec.

The NFCD is almost invariably characterized by a negative rotation of the head (extension) followed by a positive rotation (flexion) which distinguishes it from all other initial conditions examined in this paper.

The comparison of angular acceleration between these conditions is even more dramatic. The peak angular acceleration from the NFCD initial condition is approximately  $1/3$  of the peak angular acceleration for the NUCU condition (Fig. 11). In addition, we see that the angular acceleration for the NFCD condition is much less peaked than that for the NUCU condition.

In the extreme neck forward position obtained with the NFCD condition we probably are seeing the head motion with very little or no interaction between the head and the neck. The head behaves as if it were responding to moments around the effective hinge point of the head to the neck. This has important implications as to where the hinge point is in the anatomy and what the model should be for other initial conditions but these arguments have not been quantified at the time of this paper.

Comparison of the horizontal acceleration profiles at the  $T_1$  origin indicate about the same first peak values but the subsequent oscillation or notch in the profile appears attenuated in the NFCD condition relative to the NUCU condition. In a qualitative sense, the attenuation of this notch is in evidence on a majority of runs in the NFCD condition. Since the angular acceleration and angular velocity are also much attenuated for this condition, it suggests that at least a part of this observed notch characteristic might be due to head feedback on  $T_1$ .

A comparison of the resultant accelerations indicate a much less dramatic change in shape between the two conditions and a much less pronounced change in peak values.

The profiles for the NFCD and NUCD condition are not shown since they are very similar in shape to the NUCU condition differing mainly in peak values.

A comparison of the peak values for all the conditions for each subject is shown for the 6G and 10G runs in Tables 4 and 5

LX0739	RM20XS = (+)	H00041 NFCD	100.	7895.8
LX0567	RM20XS = (.)	H00041 NUCU	100.	7281.1

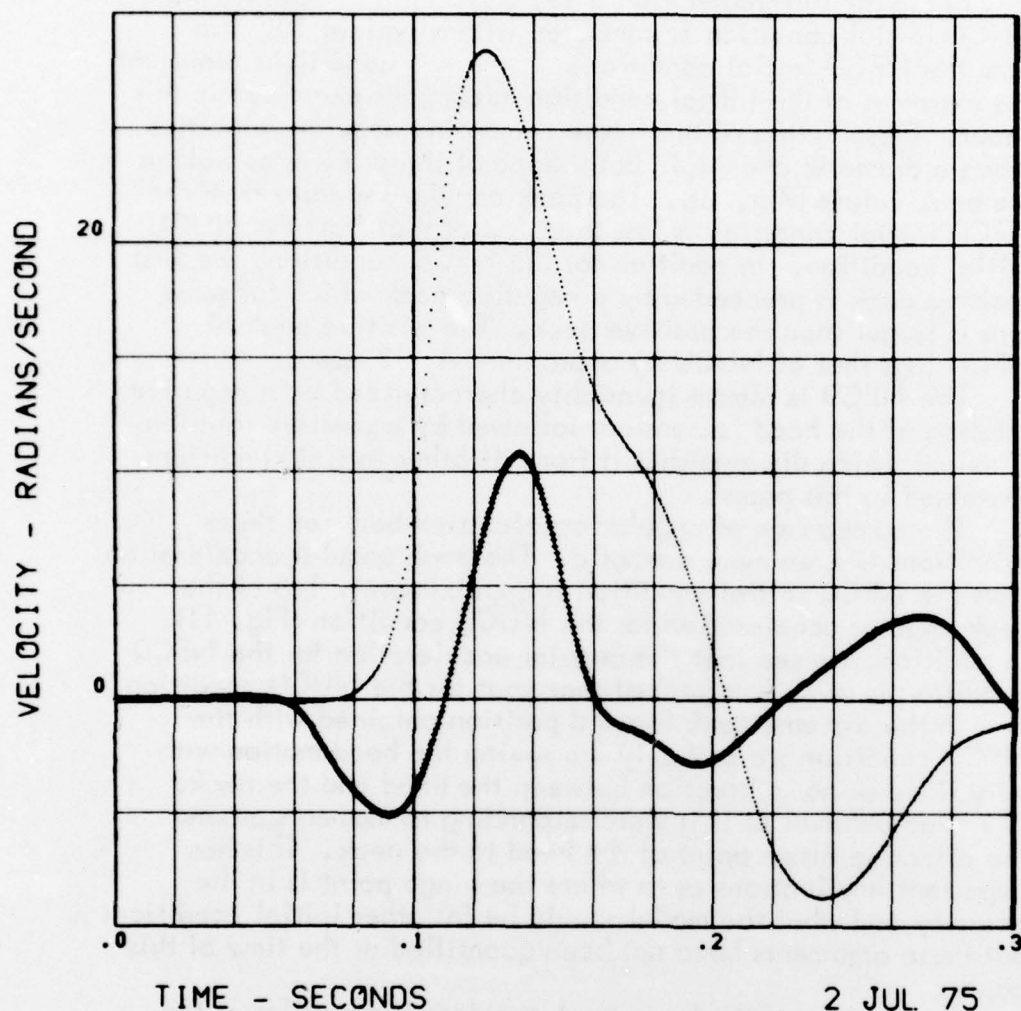


Fig. 10 - Comparison of angular velocity for NUCU versus NFCD initial conditions (10G peak sled acceleration)

respectively. Again, it is emphasized that the description for condition only agrees in an average sense with the actual measured angles. Observation of the averages for the 6G runs and 10G runs indicate that with regard to angular velocity and angular acceleration the peak values from largest to smallest are for conditions NUCU, NUCD, NFCU and NFCD respectively. The order for resultant acceleration from largest to smallest is consistent between the 6G and 10G runs and is NUCU, NFCD, NUCD, and NFCU respectively. The resultant acceleration for NFCD, NUCD and NFCU however, do not differ by very much. The order for the peak values of horizontal acceleration at the  $T_1$  origin for 10G is NFCU, NUCU, NUCD and NFCD whereas for 6G NUCU is the greatest and very little difference exists between the other conditions.



LX0739	QM20XS = (+)	H00041 NFCD	100.	7895.8
LX0567	QM20XS = (.)	H00041 NUCU	100.	7281.1

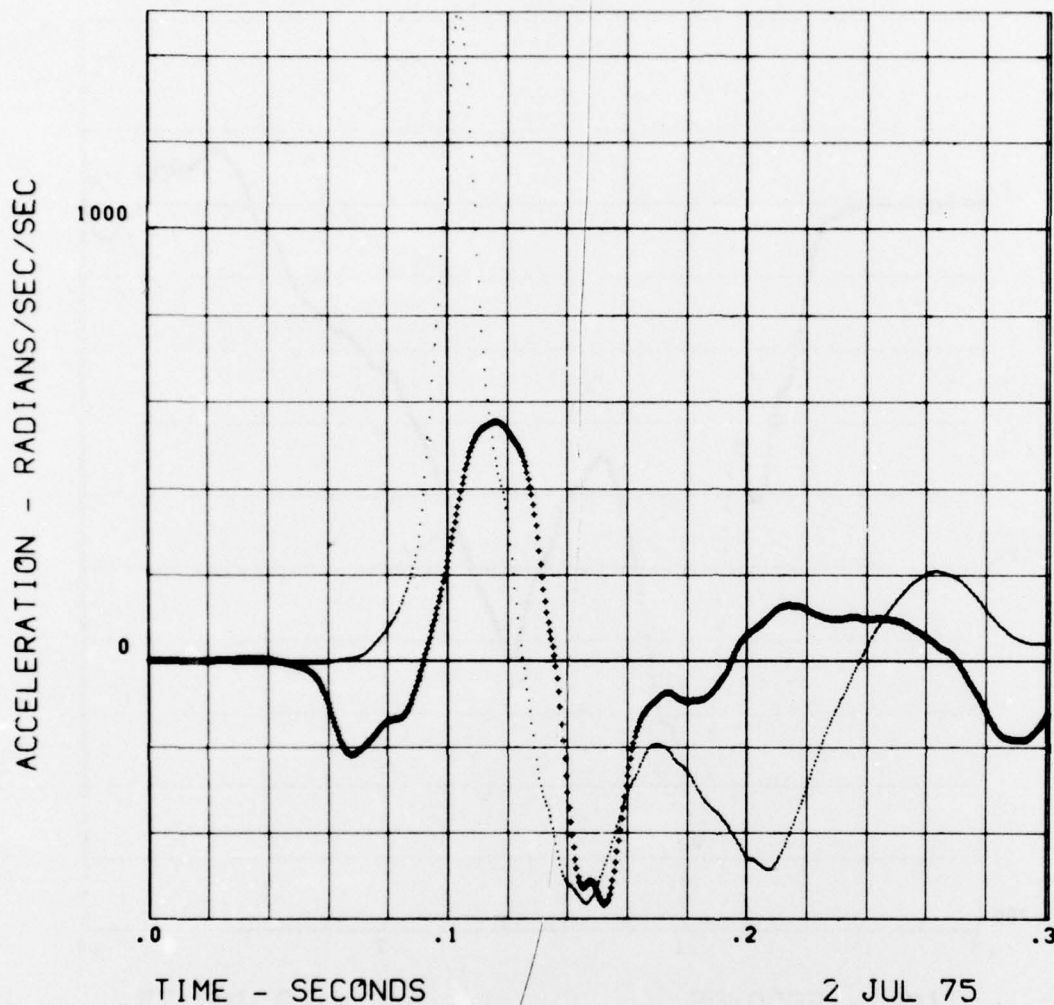


Fig. 11 - Comparison of angular accelerations for NUCU versus NFCD initial conditions (10G runs)

The data for all subjects for both 6G and 10G runs for conditions NFCD, NUCD, and NUCU were pooled and a stepwise regression program was used to determine if the data significantly regressed on neck and head angle. The NFCD condition was excluded because as mentioned previously the shape of angular acceleration and angular velocity was significantly different for this condition.

The stepwise regression program initially used all of the independent variables in the regression and then an F ratio for each coefficient based on the marginal distribution for that coefficient was calculated. The minimum F ratio was then compared to a 5% significance level threshold and the variable was eliminated from the regression if this threshold was not



LX0739	ATXX0S = (+)	H00041 NFCD	100.	7895.8
LX0567	ATXX0S = (.)	H00041 NUCU	100.	7281.1

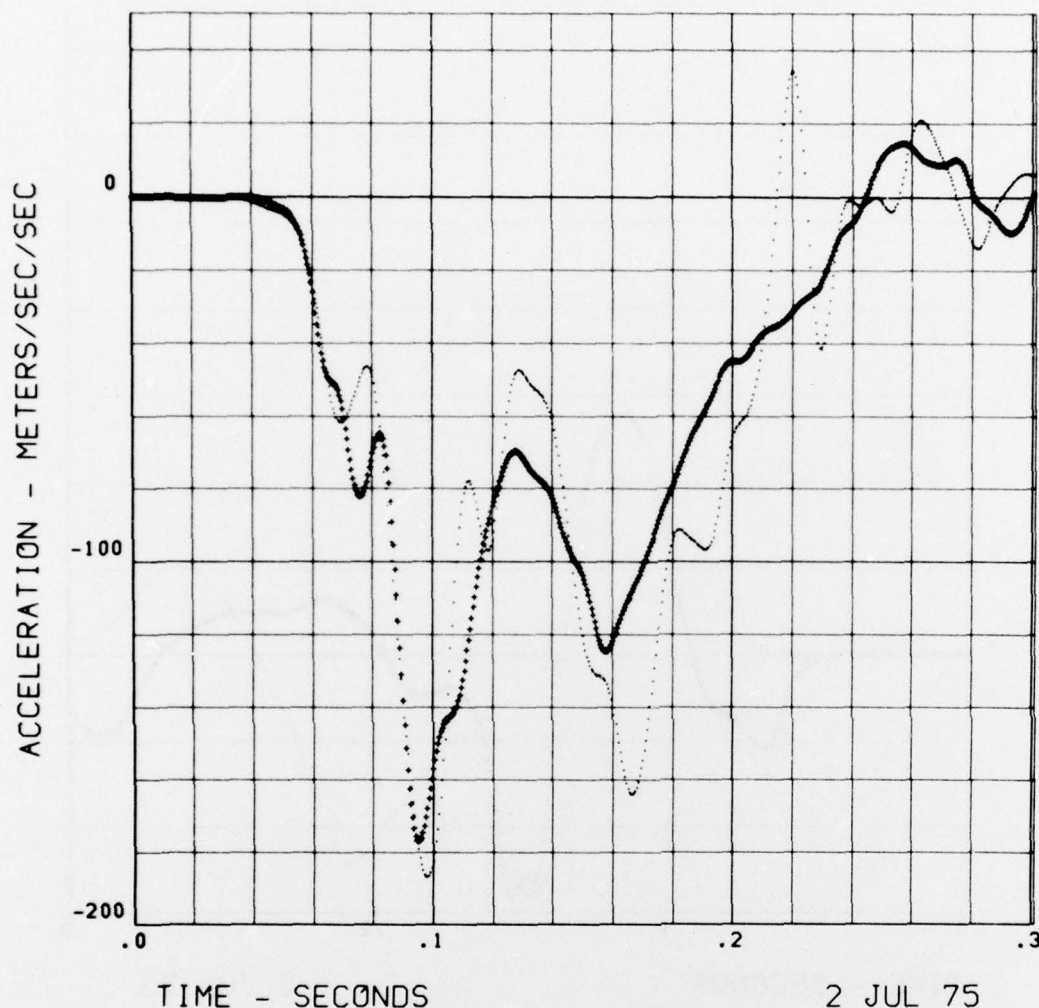


Fig. 12 - Comparison of horizontal acceleration at T1 origin for NUCU versus NFCD initial conditions (10G runs)

exceeded. The coefficients and the covariance matrix were updated and the process repeated until the F ratio for each of the remaining variables exceeded the 5% significance level.

The independent variables in the regression were as follows:

- C = Constant - dimension of dependent variable
- P.S.A. = Magnitude peak sled acceleration - G's
- ΘN = Neck angle - degrees
- ΘH = Head angle - degrees
- ATX = Magnitude of peak horizontal acceleration at the T<sub>1</sub> origin - G's. Note: Either P.S.A. or ATX were used but not both

LX0739	AMXZOS = (+)	H00041 NFCD	100.	7895.8
LX0567	AMXZOS = (.)	H00041 NUCU	100.	7281.1

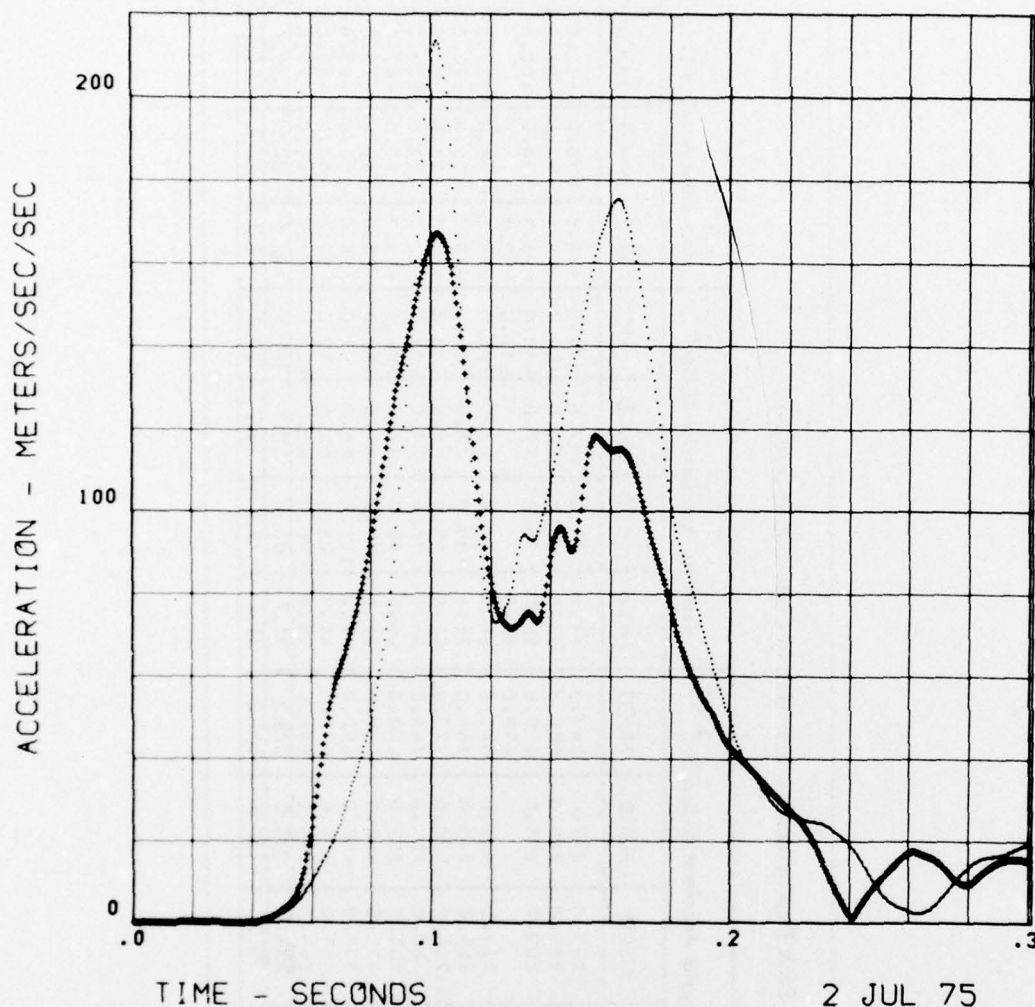


Fig. 13 - Comparison of resultant linear acceleration of head anatomical origin for NUCU versus NFCD initial conditions (10G runs)

The dependent variables were as follows:

$\omega$	= Peak angular velocity - rad/sec
$\dot{\omega}$	= Peak angular acceleration - rad/sec <sup>2</sup>
R	= Peak resultant linear acceleration - meters/sec <sup>2</sup>

A summary of the stepwise regression results are shown in Table 6. The regression coefficient and the standard deviation of the marginal distribution of each coefficient are shown. The important thing to observe in this table is that increasing the neck angle or increasing the head angle both result in a significant decrease in peak angular velocity and angular acceleration. The regression constant for head and neck angle are essentially the

Table 4 - Peak Parameters as a Function of Condition (6G runs)

Par Subj	Angular Velocity Rad/Sec				Angular Acceleration Rad/Sec <sup>2</sup>				Resultant Acceleration M/Sec <sup>2</sup>				Horizontal Accel at T1 M/Sec <sup>2</sup>			
	NFCU	NFCD	NUCD	NUCU	NFCU	NFCD	NUCD	NUCU	NFCU	NFCD	NUCD	NUCU	NFCU	NFCD	NUCD	NUCU
29	12.2	5.4	10.9	11.8	395.0	255.0	247.0	243.3	87.0	94.0	57.5	75.6	-86.0	-76.0	-72.0	-79.6
32	12.3	2.6	10.3	14.4	320.0	175.0	240.0	250.3	63.9	73.5	60.0	66.7	-68.4	-77.0	-81.5	-89.2
33	6.7	1.8	11.3	13.1	293.0	200.0	405.0	670.0	92.0	93.0	97.0	139.0	-93.1	-90.0	-100.0	-95.5
34	11.1	15.6	15.6	15.6	230.0	217.0	421.0	490.0	56.5	87.0	83.0	111.0	-90.8	-118.0	-130.0	-149.9
35	7.5	2.8	12.7	14.1	181.0	217.0	421.0	551.0	65.0	87.0	83.0	104.0	-95.6	-118.0	-117.5	-149.9
37	11.2	1.8	10.4	11.8	295.0	145.0	245.0	358.0	75.5	99.0	73.0	84.0	-83.1	-95.0	-75.0	-83.9
38	12.2	2.7	14.6	12.3	415.0	206.0	578.0	472.0	61.0	99.0	84.5	75.0	-74.3	-92.0	-70.0	-82.0
39	9.9	3.9	13.1	17.2	245.0	80.0	307.0	765.0	68.0	78.0	77.0	127.5	-72.2	-77.0	-107.0	-117.0
41	17.1	3.1	13.7	18.3	433.0	200.0	392.0	660.0	60.6	77.0	87.0	105.0	-74.7	-77.0	-87.0	-112.8
42	11.4	1.0	11.4	15.3	275.0	135.0	446.0	620.0	81.8	87.0	85.0	140.0	-83.7	-80.0	-79.0	-76.0
43	11.5	9.2	15.7	17.2	325.0	335.0	455.0	660.0	66.0	101.0	88.0	97.0	-76.0	-103.0	-87.0	-77.0
44	11.4	5.3	14.6	16.2	307.0	315.0	575.0	570.0	80.3	83.5	88.0	87.0	-87.0	-80.0	-89.0	-97.0
45	8.8	3.1	9.0	16.6	245.0	245.0	195.0	564.6	74.8	90.0	67.0	103.5	-89.5	-85.0	-77.0	-160.0
Mean	10.4	3.5	12.3	15.0	303.0	209.0	375.5	528.8	71.7	88.5	78.9	101.1	-82.6	-87.5	-86.8	-103.8
Std Dev	3.6	2.0	2.1	2.13	73.7	72.7	129.5	162.0	11.1	9.2	12.2	23.8	8.7	12.9	14.6	28.1



Table 5 - Peak Parameters as a Function of Condition (10G runs)

Par	Angular Velocity Rad/Sec				Angular Acceleration Rad/Sec <sup>2</sup>				Resultant Acceleration M/Sec <sup>2</sup>				Horizontal Accel at T1 M/Sec <sup>2</sup>			
	NFCU	NFCD	NUCD	NUCU	NFCU	NFCD	NUCD	NUCU	NFCU	NFCD	NUCD	NUCU	NFCU	NFCD	NUCD	NUCU
29	19.8	8.2	20.2	20.7	830.0	700.0	675.0	1010.0	157.7	194.0	145.0	208.0	-168.3	-178.0	-181.0	-173.0
32	18.9	1.6	20.3	27.2	575.0	253.0	490.0	1110.0	137.5	135.0	130.0	166.0	-177.0	-140.0	-200.0	-172.0
33	21.2	5.1	16.2	25.1	900.0	418.0	630.0	1710.0	179.0	208.0	137.0	284.0	-207.0	-161.7	-190.0	-190.0
34	22.9			27.6	901.4			1285.0	193.9			194.0	-221.8			-187.0
35	17.2	13.4	24.7	22.4	500.0	725.0	1255.0	1060.0	186.0	202.0	199.0	197.0	-251.0	-257.3	-230.0	-281.0
37	17.3	7.9	16.4	24.3	566.0	530.0	455.0	970.0	184.5	199.0	129.0	168.0	-185.5	-165.0	-164.0	-167.0
38	21.0	9.2	25.5	25.0	770.0	590.0	1100.0	1070.0	158.0	156.0	192.0	165.5	-149.0	-162.0	-182.0	-158.0
39	22.2	5.2	24.1	32.0	765.0	535.0	1110.0	1680.0	169.0	172.0	192.0	222.0	-183.0	-150.0	-199.0	-223.0
41	27.2	10.8	26.6	28.4	965.0	555.0	935.0	1500.0	165.0	167.0	157.0	214.0	-230.0	-177.0	-134.0	-192.0
42	15.1	5.8	23.4	23.7	560.0	470.0	1000.0	1125.0	157.0	149.0	225.0	174.0	-199.0	-128.0	-177.0	-188.0
43	24.5	14.0	30.0	28.2	975.0	620.0	1270.0	1370.0	163.0	142.0	198.0	182.0	-250.0	-144.0	-164.0	-118.9
44	20.7	13.3	25.7	23.5	713.0	735.0	1120.0	940.0	160.0	150.0	167.0	212.0	-191.0	-131.6	-160.0	-185.0
45	9.3	5.7	13.4	21.6	445.0	475.0	485.0	1070.0	170.0	169.0	147.0	204.0	-218.0	-222.0	-152.0	-171.0
Mean	20.0	8.4	22.2	25.4	728.1	550.5	877.1	1223.0	167.7	170.3	167.3	199.3	-202.4	-168.4	-177.8	-185.1
Std Dev	4.6	3.9	4.9	3.2	168.5	138.9	310.8	263.5	15.1	25.1	31.3	32.0	30.9	37.8	25.5	37.3



Table 6 - Regression Constants (pooled 6 and 10G runs for condition NFCU, NUCD, and NUCU)

DEPENDENT VARIABLE	INDEPENDENT VARIABLES					STD. DEVIATION OF DEPEND. VARIABLE
	CONSTANT	P.S.A.	ATX	NECK ANGLE	HEAD ANGLE	
$\omega$	-	2.53		-.111	-.152	2.90
	-	.0718		.0200	.0315	
$\dot{\omega}$	- 241.0	135.0		-7.04	-5.43	224.4
	111.9	12.39		1.66	2.46	
R	- 53.2	22.42		-	-	26.4
	12.24	1.44		-	-	
$\omega$	9.46			.793	-.108	3.84
	1.40			.0782	.0283	
$\dot{\omega}$	231.0			-43.9	-7.01	259.1
	93.8			5.23	1.90	
R	-			9.02	-	31.0
	-			.232	-	
ATX	5.19	2.36		-	-	2.81
	1.30	.153		-	-	

REGRESS. COEF.

STD DEVIATION

same whether peak sled acceleration or peak horizontal acceleration at  $T_1$  are used as independent variables. The peak resultant acceleration does not regress on neck or head angle nor does the peak horizontal acceleration at  $T_1$ . We also separated the 6G and 10G runs and solved for the regression coefficients for neck angle and head angle. Although there was an increased effect of both of these parameters with an increase in peak sled acceleration the difference was not significant at the 5% level.

The regression on peak sled acceleration of each of the three initial conditions (NFCU, NUCD, NUCU) were compared. There is no significant difference between the NFCU and NUCD condition but the NUCU condition has a significantly higher value for both peak angular velocity and angular acceleration than either of the other conditions.

The effect of increasing the neck angle was expected from our model studies as there is a decreased torque on head and neck system. The decrease of angular acceleration and velocity with increasing head angle is not consistent with our current modeling effort and bears a much closer look.

## CONCLUSIONS

1. Increasing the neck angle reduces significantly the peak angular velocity and angular acceleration when regressed on peak sled acceleration, neck angle and head angle.

2. Increasing the head angle (chin down) significantly decreases the peak angular velocity and angular acceleration when regressed on peak sled acceleration, neck angle and head angle.

3. The horizontal acceleration at the T<sub>1</sub> origin regresses on peak sled acceleration but not on neck or head angle.

4. The resultant acceleration at the head anatomical origin does not regress on neck or head angle.

5. If the peak magnitude of the T<sub>1</sub> horizontal acceleration is substituted for peak sled acceleration as an independent variable the regression constants for neck and head angle remain about the same as with peak sled acceleration. However, the regression of angular acceleration on head angle is not significant at 5% level.

6. The effect of neck angle and head angle are both greater at 10G than at 6G peak sled accelerations but the difference is not significant at 5% level.

7. The extreme initial condition (NFCD) is significantly different in shape than all the other initial conditions run. The maximum positive peaks in angular velocity and angular acceleration are preceded by a negative peak that often exceeds the positive peak in magnitude. However, whether one considers the positive or negative peak the magnitude is severely reduced when compared to the NUCU condition or for that matter when compared with any other condition. It appears that for this condition one is observing the head motion with little or no head-neck interaction.

#### ACKNOWLEDGEMENTS

Major funding and support for this work was provided by the Naval Medical Research and Development Command and research contracts and other valuable assistance by the Biological Sciences Division, Office of Naval Research. Invaluable assistance and funding was also furnished by the U. S. Army Medical Research and Development Command.

Opinions or conclusions contained in this report are those of the authors and do not necessarily reflect the views or the endorsement of the Navy Department.

Trade names of materials or products of commercial or non-government organizations are cited only where essential to precision in describing research procedures or evaluation of results. Their use does not constitute official endorsement or approval of the use of such commercial hardware or software.

The authors wish to express their appreciation to the entire staff at NAMRL Detachment and especially acknowledge the assistance of Gerald Williamson and Robert Martin of the Data Processing Division and Gayle Carp of QEI, Inc. for their contributions in processing the large quantity of data examined and presented.

Dist. AVAIL. and/or SPECIAL		
A		

☒ FOR  
☐ OR  
☐  
 CODES

## REFERENCES

1. C. L. Ewing, D. J. Thomas, G. W. Beeler, L. M. Patrick and D. B. Gillis, "Dynamic Response of the Head and Neck of the Living Human to -Gx Impact Acceleration." Paper 680792, Proceedings of Twelfth Stapp Car Crash Conference, p. 26. New York: Society of Automotive Engineers, Inc., 1968.
2. C. L. Ewing, D. J. Thomas, L. M. Patrick, G. W. Beeler, and M. J. Smith, "Living Human Dynamic Response to -Gx Impact Acceleration. II. Accelerations Measured on the Head and Neck." Paper 690817, Proceedings of Thirteenth Stapp Car Crash Conference P-28. New York: Society of Automotive Engineers, Inc., 1969.
3. C. L. Ewing and D. J. Thomas, "Human Dynamic Response to -Gx Impact Acceleration." AGARD Conference Proceedings, AGARD-CP-88-71, Oporto, Portugal, June 1971.
4. C. L. Ewing and D. J. Thomas, "Human Head and Neck Response to Impact Acceleration." Naval Aerospace Medical Research Laboratory Detachment, New Orleans, Monograph 21, August 1972.
5. C. L. Ewing and D. J. Thomas, "Torque versus Angular Displacement Response of Human Head to -Gx Impact Acceleration." Paper 730976, Proceedings of Seventeenth Stapp Car Crash Conference, New York: Society of Automotive Engineers, Inc., 1973.
6. E. B. Becker, "Preliminary Discussion of an Approach to Modeling Living Human Head and Neck Response to -Gx Impact Acceleration." Human Impact Response, Ed. W. F. King and H. J. Mertz, New York: Plenum Press, pp 321 - 329, 1973.
7. R. G. Snyder, Personal Communication, 1973.
8. G. Clauser, and K. Kennedy, "An Inquiry into the Ranges of Values Existing in the U. S. Navy Acceleration Study." 6570th Aerospace Medical Research Laboratory, Wright-Patterson Air Force Base, Ohio, April 1975, Unpublished.
9. E. C. Gifford, J. R. Provost and J. Lazo, "Anthropometry of Naval Aviators, 1964." NAEC-ACEL Report 533, Naval Air Engineering Center, Aerospace Crew Equipment Laboratory, Philadelphia, PA, 1965.
10. E. Becker and G. Willems, "An Experimentally Validated 3-D Inertial Tracking Package for Application in Biodynamic Research." Submitted to the Nineteenth Stapp Car Crash Conference, San Diego, CA, Society of Automotive Engineers, Inc., November 1975.
11. D. J. Thomas, "Specialized Anthropometry Requirements for Protective Equipment Evaluation", AGARD Conference Proceedings No. 110, Current Status in Aerospace Medicine, Glasgow, Scotland, September 1972.
12. E. Becker, "A Photographic Data System for Determination of 3-Dimensional Effects on Multi-axes Impact Acceleration on Living Humans." Submitted to Automotive Safety Seminar of the Society of Photo-Optical Instrumentation Engineers, December 1974.